Article

Investigation of Broadband Optical Nonlinear Absorption and Transient Dynamics in Orange IV Containing Azobenzene

Quanhua Wu [1], Rui Ruan [1], Xingxing Li [1], Yujie Zhao [1], Yang Li [1], Yu Fang [1], Yongqiang Chen [1], Quanying Wu [1] , Yinglin Song [2,3,*] and Xingzhi Wu [1,]**

[1] Jiangsu Key Laboratory of Micro and Nano Heat Fluid Flow Technology and Energy Application, School of Physical Science and Technology, Suzhou University of Science and Technology, Suzhou 215009, China
[2] Department of Physics, Soochow University, Suzhou 215123, China
[3] Department of Physics, Harbin institute of technology, Harbin 150001, China
* Correspondence: ylsong@hit.edu.cn
** Correspondence: wuxingzhi@usts.edu.cn

Abstract: Broadband reverse saturable absorption is systematically investigated via Z-scan, transient absorption spectrum (TAS). The excited state absorption and negative refraction of Orange IV are observed in the Z-scan experiment at 532 nm. Meanwhile, two-photon induced excited-state absorption and pure two-photon absorption are observed at 600 nm and 700 nm with the pulse width of 190 fs, respectively. An ultrafast broadband absorption in visible wavelength region is observed via TAS. The different nonlinear absorption mechanism at multiple wavelengths is discussed and interpreted from the results of TAS. In addition, the ultrafast dynamics of negative refraction in the excited state of Orange IV is investigated via degenerate phase object pump probe, from which the weak long-lived excited state is extracted. All studies indicate that Orange IV has the potential to be further optimized into a superior broadband reverse saturable absorption material and also has certain reference significance for the study of optical nonlinearity in organic molecules containing azobenzene groups.

Keywords: Nonlinear optics; Z-scan; Transient absorption and refraction; Pump probe

1. Introduction

The decades of progress in nonlinear optics research have been accompanied by the development of applications such as harmonic generation [1], broadband reverse saturation absorption [2-3], and all-optical switching [4]. For the realization of these unique applications, nonlinear optical materials are indispensable. Among them, broadband reverse saturable absorption materials are considered to have important application potential in the protection of ultrashort pulse laser. Thus, organic nonlinear materials are widely concerned because of their large optical nonlinearity, broad spectral response and easy modification. The optical nonlinear response of organic materials is decisively related to the off-domain π-electrons within the π-conjugated system of the molecule. The azobenzene group has a fast nonlinear optical response and a large nonlinear optical (NLO) coefficient due to its large π-conjugated system [5-8]. The NLO properties of the azobenzene group have broad application prospects in photorefractive, optical communication and magnetic memories materials [9-11]. Meanwhile, azobenzene and its derivatives, due to their trans and cis isomerization, thus constitute a series of important photonic switches [12-15]. The cis-trans structural isomerization further may have induced changes in the third-order NLO behavior of the molecule [16-17]. A previous report showed an enhanced NLO response at 1064 nm for some azobenzene derivative molecules associated with the cis-isomer [18]. Other reports have investigated the ability of polymer films and complexes of some azobenzene derivatives to induce two-photon absorption based on a nonlinear optical-photo isomerization cycle model [19-20]. These results demonstrate the value of azobenzene-containing organic molecules for applications in nonlinear optics research. However, most of the studies focus on the photoisomerization process of azobenzene

Preprints (www.preprints.org) | NOT PEER-REVIEWED | Posted: 25 April 2023 doi:10.20944/preprints202304.0890.v1

and its derivatives, with little attention paid to the broadband nonlinear absorption and transient refraction of molecules containing azobenzene groups.

Here in this work, the broadband nonlinear optical absorption of an azobenzene containing molecule (Orange IV) at multiple wavelengths are investigated by femtosecond Z-scan, and results indicate that the sample exhibits reverse saturation absorption (RSA) at 532 nm, and two-photon induced excited state absorption (TP-ESA) is observed at 600 nm, while two-photon absorption (TPA) is observed at 700 nm. The different nonlinear absorption mechanisms at various wavelengths are successfully verified and explained by TAS, which is in good agreement with the results of femtosecond Z-scans at multiple wavelengths. Besides, RSA and negative refraction of the excited state is observed at 532 nm with various pulse width lasers (including 190 fs, 13 ps, 4 ns). The ultrafast dynamics of negative refraction in the excited state of Orange IV is investigated via degenerate phase object pump probe, from which the weak long-lived excited state is extracted. These results provide some reference to the research of the optical nonlinearity of some organic molecules containing azobenzene.

2. Results and Discussion

2.1 UV-vis absorption and fluorescence

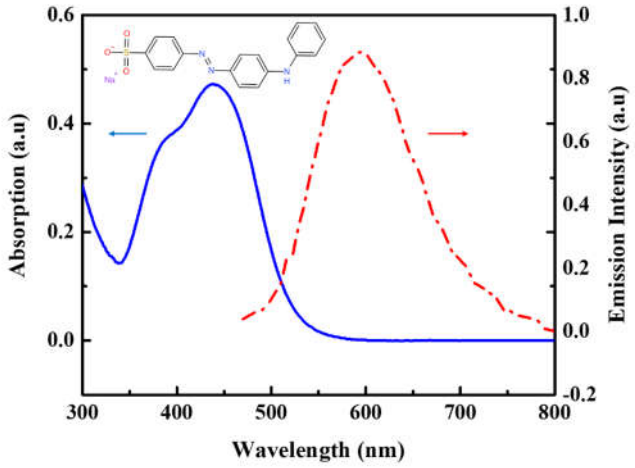

Figure 1. UV-vis absorption (blue) and fluorescence (red) spectra of Orange IV. The concentrations of Orange IV are 2.66×10^{-5} M in dimethyl sulfoxide（DMSO）solution.

We monitored the UV-vis absorption and fluorescence spectrum of Orange IV at room temperature. As shown in Figure 1, the strong visible absorption band arises at the wavelength of 436 nm. At the same time, the fluorescence emission peak corresponding to the absorption peak appears at the 591 nm wavelength in the detection window. Comparing the UV-vis and fluorescence spectrum, we can find that the absorption and emission peaks agree with the mirror image rule, indicating that the absorption signal may originate from the first singlet state [21-23].

In order to obtain more linear absorption information, DFT calculations are conducted as shown in Figure 2. It can be found that there is a visible charge transfer in the left benzene ring under excitation. The calculated energy gap between HOMO and LUMO is 2.921eV, which corresponds to a wavelength of 425 nm, very close to the absorption peak of Orange IV solution at 436 nm. These results indicate that the sample has a visible intramolecular charge transfer (ICT) feature.

Preprints (www.preprints.org) | NOT PEER-REVIEWED | Posted: 25 April 2023 doi:10.20944/preprints202304.0890.v1

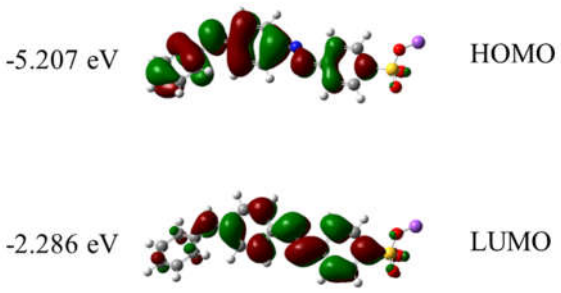

Figure 2. Electron distribution and energy of frontier molecular orbitals in Orange IV.

2.2 The third-order NLO research

To evaluate the third-order optical nonlinearity of Orange IV, Z-scan measurements are conducted under various pulse widths. The calibration of the extracted data can be significantly improved by using 3 mm thickness zinc selenide as a standard sample. The Z-scan with open aperture (OA) reflects the nonlinear absorption of the sample, while the closed aperture (CA) Z-scan reflects the non-linear refraction of the sample. Femtosecond Z-scan experiments were conducted at 532nm, 600nm and 700nm, respectively. When excited with 532 nm laser pulses (incident laser intensity of 21.4 GW/cm^2), the OA Z-scan (Figure3(a)) of Orange IV displays a single valley at zero position (focal point), indicating the lower transmittance under higher laser intensity, which is a typical feature of reverse saturable absorption. In addition, the CA Z-scan curve (Figure3(b)) of the sample after the removal of the solvent background (as shown in FigureS1) displays the shape of a peak followed by a valley, suggesting a negative change of the nonlinear refractive index as the sample moves from the -z to +z position, referred to as the self-defocusing effect. Considering that 532 nm is located within the edge of the linear absorption band and the linear transmittance of the sample is 0.35 (excluding the reflection of cuvette), both the RSA and the negative nonlinear refraction (NLR) under resonant excitation could be attributed to the excited state optical nonlinear response.

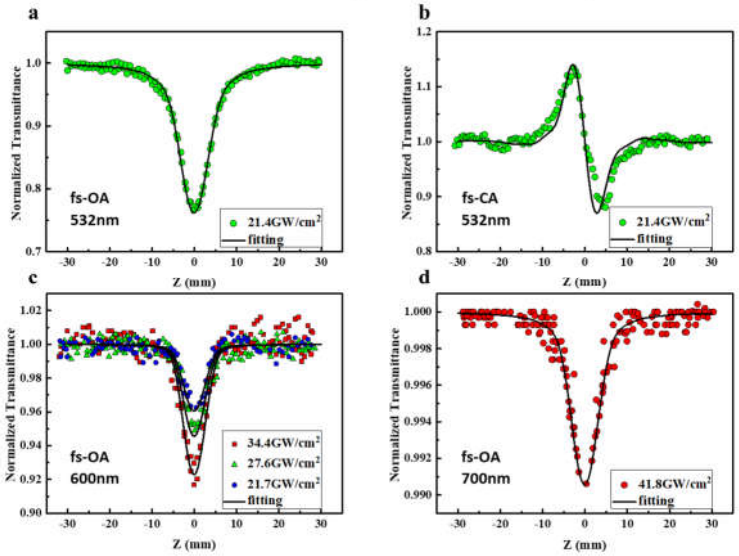

Figure 3. Femtosecond Z-scan measurement curve of Orange IV. (a) Open aperture curve at 532 nm. (b) Closed aperture curve at 532 nm. (c) and (d) Open aperture curve at 600 nm and 700 nm. Solid line represents the results of numerical fitting.

When tuning the laser incident wavelength to a non-resonant absorption band, Orange IV exhibits an extremely high linear transmittance of 0.93 at 600 nm and 700 nm (almost identical to linear transmittance of the pure solvent DMSO). The OA Z-scan curves

Preprints (www.preprints.org) | NOT PEER-REVIEWED | Posted: 25 April 2023 doi:10.20944/preprints202304.0890.v1

of Orange IV at both 600 nm and 700 nm similarly record a single valley, as shown in Figure3(c) and (d). Unlike the case of 532 nm, as the 600 nm and 700 nm wavelengths are away from the resonant absorption band, the nonlinear absorption (NLA) at both wavelengths cannot originate from single photon induced excited state absorption, so we assign the NLA to multi-photon absorption. It should also be noted that after eliminating the effect of positive refraction from the solvent background, NLR was not observed in Orange IV solution at both wavelengths, which is different from the negative refraction at 532 nm.

Numerical simulations based on Sheik Bahae's theory are used to fit the results from the Z-scan experiment, where the nonlinear absorption coefficient and refractive index of the sample are expressed as:

$$\alpha = \alpha_0 + \beta I + (\gamma I^2) \quad (1)$$

$$n = n_0 + n_2 I \quad (2)$$

where α_0 is linear absorption coefficient, β and γ are effective nonlinear absorption coefficients for third-order and fifth-order, respectively. If only third-order nonlinear absorption exists in the sample, γ is zero. Similarly, n_0 and n_2 represents the linear refractive index and third-order nonlinear refractive index, respectively. The numerical simulation curve is the solid black line in Figure3.

As discussed above, the optical NLA and NLR at 532 nm wavelength are mainly determined by excited state absorption and refraction. As for the 600 nm case, at different peak intensities including 21.7 GW/cm^2, 27.6 GW/cm^2, and 34.4 GW/cm^2, the corresponding third-order nonlinear coefficients β are 1.3×10^{-13} m/W, 1.6×10^{-13} m/W and 2.0×10^{-13} m/W, respectively, which are almost proportional to the incident intensity. This suggests that there may be a higher order NLA at 600 nm. The $\gamma(I^2)$ term is then additionally taken into account in our absorption coefficients, giving third- and fifth-order nonlinear absorption coefficients β and γ independent of the incident intensity (listed in Table 1), which matched the experimental data well. It is noted that the 600 nm wavelength is in the non-resonant absorption band, but it is unlikely to absorb three photons at this wavelength at the same time. Therefore, the RSA is more likely to originate from TP-ESA. However, the NLA was observed at an incident intensity of 41.8 GW/cm^2 when the sample was excited at 700 nm, and effective NLA signals cannot be extracted from the noisy background at lower intensities. Noting that the energy of two 700 nm photons is equivalent to the energy of a single photon at 350 nm, and yet the linear absorption at 350 nm is weaker as seen in Figure1, thus the NLA here can be considered to be purely dominated by TPA. The nonlinear parameters for the different wavelengths in the femtosecond Z-scan are listed in Table 1.

Table 1. Nonlinear parameters of femtosecond Z-scan experiment.

	532 nm, T=0.35	600 nm, T=0.93	700 nm, T=0.93
Orange IV	β= 2.2×10^{-12} m/W	β= 4.4×10^{-14} m/W	β= 2.5×10^{-14} m/W
	n_2= -6.5×10^{-20} m^2/W	γ= 6.3×10^{-28} m^3/W^2	–

Furthermore, as shown in Figure4, picosecond and nanosecond Z-scans are also implemented at 532 nm with incident laser intensities of 2.7 GW/cm^2 and 38.2 MW/cm^2, corresponding to β of 1.6×10^{-11} m/W and 3.8×10^{-10} m/W, and n_2 of -2.5×10^{-18} m^2/W and -6.3×10^{-17} m^2/W, respectively. Similar to the femtosecond Z-scan at 532 nm, the Orange IV molecules also exhibit single photon induced RSA and negative refraction.

Preprints (www.preprints.org) | NOT PEER-REVIEWED | Posted: 25 April 2023 doi:10.20944/preprints202304.0890.v1

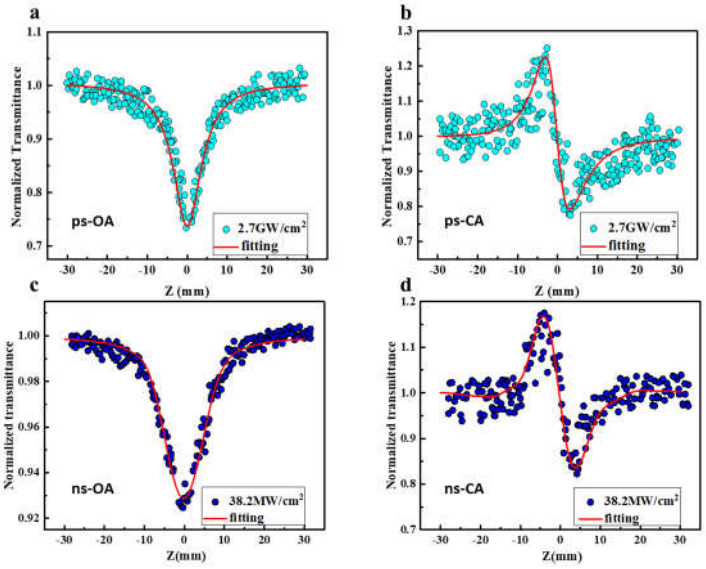

Figure 4. The open and closed aperture picosecond (a, b) and nanosecond (c, d) Z-scan curves of Orange IV under 532 nm. The solid line represents the theoretical fitting.

2.3. Transient absorption spectrum

The results of the Z-scan indicate that different absorption mechanisms play a key role in the optical nonlinearity of Orange IV. To further distinguish and explain the differences of the NLA at various incident laser wavelengths, transient absorption spectrum is conducted in the visible region.

The TAS is recorded and displayed in Figure5(a) with the probe window ranging from 505-750 nm. It is clear that the broadband RSA of the sample covers the entire detection wavelength region. In addition, for more details, we extract spectral curves at different delay times, which are shown in Figure5(b). The recorded ultrafast broadband excited state absorption builds up within a pulse width. Moreover, the excited state absorption (ESA) signal increases in the range of approximately 505-630 nm and decreases in the range of 630-750 nm as the absorption spectrum with a time delay of 0.2 ps evolves to that of 0.4 ps. After that, the spectral curve decays in a similar shape with a very short time. Considering the spectrum curve with a lifetime of 0.2 ps (about one pulse width) and femtosecond Z-scan, the excited state absorption is found at 532 nm and 600 nm, which explains the existence of single photon induced excited state absorption and TP-ESA at 532 nm and 600 nm, respectively, while the ESA signal at 532 nm is stronger than that at 600 nm, which is consistent with the results of femtosecond Z-scan. Furthermore, the excited state absorption found at 700 nm is comparatively little, which may be the reason that TPA at 700 nm could not trigger the subsequent excited state absorption as at 600 nm.

The global analysis [24] is used to numerically reconstruct the TAS. The TAS could be divided into different components for a reasonable fit, and each component has a featured absorption spectrum ($A_n(\lambda)$) and a corresponding decay lifetime. Thus, the entire TAS could be expressed as:

$$F(t,\lambda) = \sum_n N_n(t) \times A_n(\lambda) \quad (3)$$

Where $F(t, \lambda)$ stands for the reconstructed TAS and N_n(t) represents for the population density of the excited states that change with time. Each excited state energy level corresponds to a spectral component $A_n(\lambda)$, which is expressed as a single e-exponential function with lifetime τ. The lifetimes of a total of two components are used to reasonably fit the TAS. The spectral components extracted from the global analysis are shown in Figure5(c). The lifetimes of the two components extracted from the simulations are 0.3 ps, 4.1 ps, respectively. The numerical simulation results of the dynamics for the corresponding wavelengths used in the Z-scan are plotted in Figure5(d). Ultrafast locally excited state absorption is established at femtosecond laser incidence and then departure from the local excited state (LE) [19, 25] with a lifetime of 0.3 ps, accompanied by relaxation to the charge transfer

Preprints (www.preprints.org) | NOT PEER-REVIEWED | Posted: 25 April 2023 doi:10.20944/preprints202304.0890.v1

state (CT). The slower component with a lifetime of 4.1 ps is attributed to the relaxation of the CT state, and the slower decay lifetime may be related to the photoisomerization process in terms of previous reports [26-27].

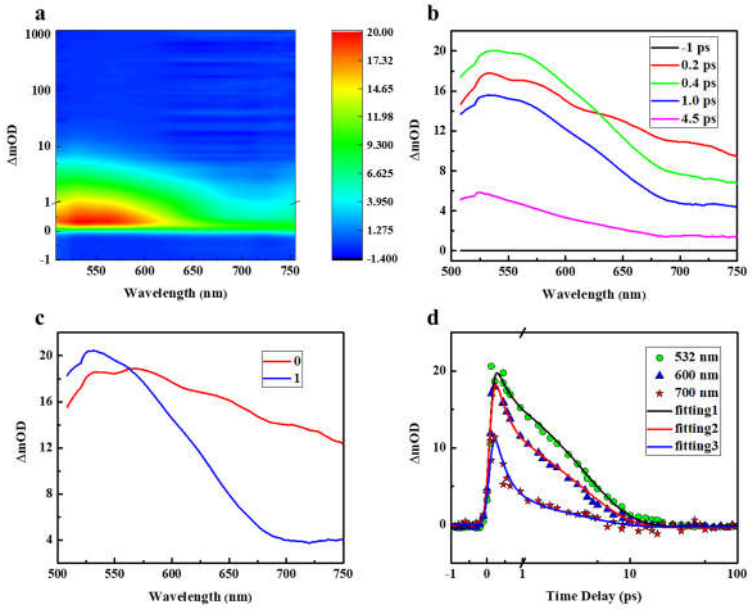

Figure 5. Results of transient absorption spectra of Orange IV solutions. (a) A 2D color map of transient absorption experiment. (b) TAS under different delay times. (c) Spectral components extracted from global analysis. (d) Numerically fitted kinetic curves at various wavelengths.

2.4. Ultrafast excited state refraction

It is also interesting to note that Orange IV still exhibits negative NLR from the excited state in the Z-scan results under 532 nm. Since negative nonlinear optical refraction could be applied to all-optical switching [28-29]. The dynamics of NLA and NLR are investigated via a degenerate phase-object pump-probe (POPP) technique. POPP technology enables simultaneous measurement of NLA and refraction by transforming nonlinear refractive index changes into transmittance changes via phase objects, and can detect transmittance changes with an accuracy of 0.02. The sample solution is pumped and probed at 515 nm. The POPP results are shown in Figure6.

The NLA dynamics in Figure 6(a) shows a strong RSA at zero time followed by a decrease with the lifetime of 0.3 ps and 4.1 ps, which is in good agreement with the kinetic results in the TAS. Moreover, the long-lived weakly excited state absorption (Normalized transmittance of about 0.98) is extracted in Figure 6(c), which indicates that the absorption cross section of the excited state is slightly larger than that of the ground state (S_0). This long-lived relaxation process of excited states may originate from vibration cooling of the ground state. The excited state energy level slightly larger than the ground state absorption cross section is defined as S_{vib}, and the relaxation lifetime of this excited state is more than 4 ns. This explains the OA nanosecond Z-scan results. Correspondingly, the dynamics of the NLR (Figure 6(b, d)) begins with an ultrafast rise in positive refraction near zero time, which originates from the Kerr refraction of the solvent background. After that, the dynamics of NLR display an ultrafast drop, which indicate the strong negative excited-state NLR in Orange IV solution. This is immediately followed by an ultrafast recovery process with nonlinear negative refraction, in which there are two decay lifetimes of 0.3 ps and 4.1 ps, corresponding to the relaxation of the local excited state and charge-transfer state in transient absorption dynamics, respectively. Finally, the transient refraction profile of Orange IV exhibits weak negative refraction and is maintained for a long time,

Preprints (www.preprints.org) | NOT PEER-REVIEWED | Posted: 25 April 2023 doi:10.20944/preprints202304.0890.v1

corresponding to the long-lived weakly excited state energy level (S_{vib}). These results are consistent with the above discussion of Z-scan with multiple pulse widths.

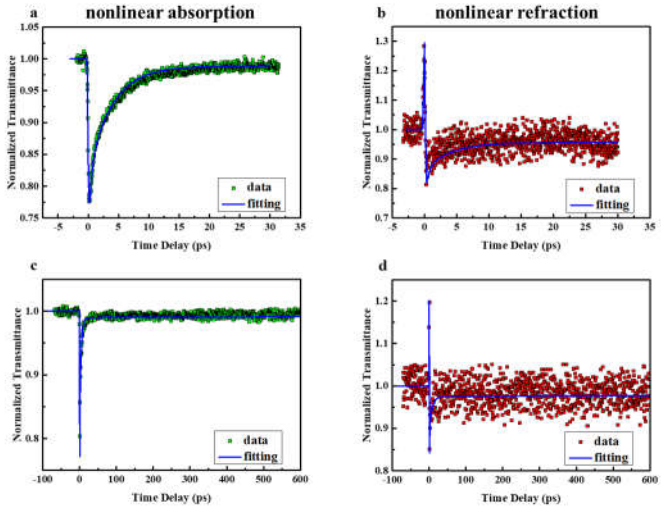

Figure 6. The transient ((a), (c)) NLA and ((b), (d)) NLR of Orange IV probed at 515 nm, measured with degenerate POPP. Solid lines represent the results of the numerical simulation.

Generally, after excitation by the pump pulses, the excited state electrons decay to each excited state in turn and finally relax to the ground state. Simplified rate equations based on the energy model are used to numerically fitting the results. the modulation of the intensity (I_p) and phase (φ_p) of the probe beam can be expressed as:

$$\frac{dI_p}{dz} = -I_p\left(\sum_{n\geq 1}\sigma_n N_n + 2\beta I_e\right) \tag{4}$$

$$\frac{d\varphi_p}{dz} = k\left(\sum_{n\geq 1}\Delta\eta_n N_n + 2n_2 I_e\right) \tag{5}$$

Where I_p and I_e represent the light intensity of the probe beam and the pump beam, and n_2 is the Kerr refractive index related to the incident intensity, which is set to n_2=6.5×10^{-19} m^2/W based on the experiment. And z represents the propagation length of the laser in the sample, σ_n stands for the absorption cross section of the excited state, $\Delta\eta_n$ is the change of refractive volume between the effective energy state and the ground state. As discussed above, the equivalent energy level model as shown in Figure 7 is built up to fit the data. Following numerical simulations, a series of parameters including excited state absorption cross sections, refractive volumes and lifetimes are fitted and listed in Table 2. It is worth noting that the lifetimes of S_{vib} state larger than 4 ns cannot be determined accurately due to the limited delay time.

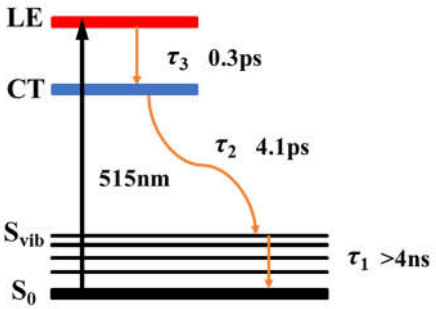

Figure 7. Simplified energy level of the excited state of Orange IV.

Preprints (www.preprints.org) | NOT PEER-REVIEWED | Posted: 25 April 2023 doi:10.20944/preprints202304.0890.v1

Table 2. Parameters of excited states extracted from the numerical simulation.

State	σ_n (m^2)	$\Delta\eta_n$ (m^3)	τ_n (ps)
LE	8.8×10^{-21}	-3.1×10^{-21}	0.3
CT	4.7×10^{-21}	-1.1×10^{-21}	4.1
S_{vib}	1.4×10^{-21}	-7.2×10^{-22}	>4000
S_0	1.2×10^{-21}	0	-

3. Materials and Methods

3.1. Characterization of Orange IV

As a general biological stain and acid-base indicator, Orange IV can be purchased from many chemical companies. The structure of Orange IV is shown in Figure1. 1H NMR (400 MHz, DMSO-d6) δ 8.89 (s, 1H), 7.82 (d, J = 8.9 Hz, 2H), 7.74 (s, 4H), 7.37 – 7.29 (m, 2H), 7.22 (d, J = 7.3 Hz, 2H), 7.17 (d, J = 9.0 Hz, 2H), 6.99 (t, J = 7.3 Hz, 1H).

3.2. Z-scan experiment

The open and closed aperture Z-scan were conducted to measure the nonlinear absorption and refractive response of Orange IV [30]. The laser source included a mode-locked Yb: KGW based fiber laser (1030 nm, Orpheus, Light Conversion.) with an output pulse width of 190 fs, a Q-switched and mode locked Nd: YAG laser (PW-1064-1B) working at 532 nm with 13 ps pulse width (FWHM) and 4 ns (FWHM) pulse of 532 nm were extracted from a Q-switched Nd: YAG laser (Surelite II, Continuum). The low repetition rate is set to 20 Hz in femtosecond and picosecond pulses and 10 Hz in nanosecond pulse to avoid thermal lens effect caused by heat accumulation of the sample [31-32]. The Orange IV is dissolved in DMSO with the concentration of 2.66×10^{-3} M and contained in a 2 mm quartz cuvette. The sample solution is placed on an electric translation platform, which is controlled by the set program and moves along the z-axis. During the movement, the experimental data is recorded by the energy detectors.

3.3. Femtosecond transient absorption spectroscopy

The transient absorption spectrum can record the ultrafast absorption and kinetic relaxation processes at different wavelengths after excitation. A detailed description of the experimental system can be seen elsewhere [33]. The femtosecond fiber laser used in the experiment is the same as in the Z-scan above, the pump pulse is tuned to 400 nm (14 mW), and the probe beam is a supercontinuum light generated from the fundamental frequency (1030 nm) via the sapphire crystal. The repetition rate of laser pulse is 6 kHz. The probe window of the grating spectrometer is adjusted to 505-750 nm.

3.4. Phase object pump-probe

The dynamic traces of ultrafast nonlinear absorption and refraction are conducted by the pump-probe technology with phase object [34]. The phase object pump-probe (POPP) technology is a combination of conventional pump-probe and 4f phase object imaging system [35], which be able to simultaneously measure the evolution of transient nonlinear absorption and refraction. The laser source used in the experiment is the same as in the TAS. The repetition frequency of laser pulse is 20 Hz. The wavelengths of pump and probe light of degenerate POPP are both 515 nm. The sample dissolved in DMSO with a concentration of 6.65×10^{-4} M is prepared in a 2 mm quartz cuvette for measurement.

3.5. Quantum chemical calculations

Quantum chemical calculations are performed on Orange IV at the level of B3LYP/6-31G (d,p) via the Gaussian 09 program package to obtain optimized structures and frontier molecular orbitals.

4. Conclusions

The broadband optical nonlinear absorption of Orange IV is investigated systematically. The strong ESA and nonlinear negative refraction at 532 nm, the TP-ESA at 600 nm, and the TPA at 700 nm are observed via the femtosecond Z-scan. Moreover, picosecond and nanosecond Z-scan also reveal that the molecules have excited state absorption and negative refraction. Ultrafast broadband excited state absorption is observed in the TAS, and the NLA mechanism of different wavelengths are verified and characterized. Besides, the long-lived weak excited state of nanosecond scale is observed, and the negative refraction dynamics of excited state response are extracted in POPP experiments, which is consistent with the results of Z-scan with multiple pulse widths. These studies suggest that Orange IV has the potential to further optimize into superior broadband reverse saturated absorption materials, and it has certain reference significance for the study of optical nonlinearity in organic molecules containing azobenzene.

Supplementary Materials: Figure S1: Closed Aperture Z-scan results of solvent DMSO and Orange IV solution at 532 nm; Figure S2: ^{1}H NMR spectrum of Orange IV in DMSO.

Author Contributions: Quanhua Wu: Investigation, Writing- Original Draft. Rui Ruan: Formal analysis. Xingxing Li: Formal analysis. Yujie Zhao: Formal analysis. Yang Li: Supervision. Yu Fang: Supervision. Yongqiang Chen: Supervision. Quanying Wu: Resources, Funding acquisition. Yinglin Song: Resources, Supervision. Xingzhi Wu: Resources, Conceptualization, Validation, Funding acquisition, Methodology.

Funding: The authors gratefully acknowledge the support of the National Natural Science Foundation of China (Grant Nos. 11804244, 11704273, 22008164), Natural Science Foundation of Jiangsu Province (No. BK20180965, BK20170375, BK20190939), Jiangsu Key Disciplines of the Fourteenth Five-Year Plan (Grant No. 2021135) and the Natural Science Foundation of the Jiangsu Higher Education Institutions of China (Grants No. 19KJB150018).

Institutional Review Board Statement: Not applicable.

Informed Consent Statement: Not applicable.

Data Availability Statement: Not applicable.

Conflicts of Interest: The authors declare that they have no known competing financial interests or personal relationships that could have appeared to influence the work reported in this paper.

References

1. Boyd, R. W. *Nonlinear Optics*, 4th ed; Academic press, USA, **2020**; pp. 4-6.
2. Bai, Y.; Olivier, J.-H.; Yoo, H.; Polizzi, N. F.; Park, J.; Rawson, J.; Therien, M. J. Molecular Road Map to Tuning Ground State Absorption and Excited State Dynamics of Long-Wavelength Absorbers. *J Am Chem Soc*. **2017**, *139*, 16946-16958.
3. Wu, X.; Xiao, J.; Sun, R.; Jin, T.; Yang, J.; Shi, G.; Wang, Y.; Zhang, X.; Song, Y. Spindle-Type Conjugated Compounds Containing Twistacene Unit: Synthesis and Ultrafast Broadband Reverse Saturable Absorption. *Adv Opt Mater*. **2017**, *5*, 1600712.
4. Gu, B.; Zhao, C.; Baev, A.; Yong, K.-T.; Wen, S.; Prasad, P. N. Molecular Nonlinear Optics: Recent Advances and Applications. *Adv Opt Photonics*. **2016**, *8*, 328-369.
5. Chu, C. C.; Chang, Y. C.; Tsai, B. K.; Lin, T. C.; Lin, J. H.; Hsiao, V. K. Trans/Cis-Isomerization of Fluorene-Bridged Azo Chromophore with Significant Two-Photon Absorbability at near-Infrared Wavelength. *Chem Asian J*. **2014**, *9*, 3390-3396.
6. He, T.; Wang, C.; Zhang, J.; Zhang, X.; Lu, X. Nonlinear Absorption in an Azo-Containing Ion Liquid Crystal Polymer in the Different Excitation Regimes. *Synthetic Met*. **2010**, *160*, 1896-1901.
7. He, T.; Cheng, Y.; Du, Y.; Mo, Y. Z-Scan Determination of Third-Order Nonlinear Optical Nonlinearity of Three Azobenzenes Doped Polymer Films. *Opt Commun*. **2007**, *275*, 240-244.
8. Pan, Y.; Wang, C. Periodic Oscillation of the Optical Transmittance in Azo Dye-Doped Liquid Crystals between Two Crossed Polarizers. *Opt Commun*. **2020**, *461*, 125225.
9. Nahata, A.; Shan, J.; Yardley, J. T.; Wu, C. Electro-Optic Determination of the Nonlinear-Optical Properties of a Covalently Functionalized Disperse Red 1 Copolymer. *JOSA B*. **1993**, *10*, 1553-1564.

10. Ushiwata, T.; Okamoto, E.; Kaino, T. Development of Thermally Stable Novel Eo-Polymers. *Mol Cryst Liq Cryst*. **2002**, *374*, 303-314.
11. Venkataramani, S.; Jana, U.; Dommaschk, M.; Sönnichsen, F.; Tuczek, F.; Herges, R. Magnetic Bistability of Molecules in Homogeneous Solution at Room Temperature. *Science*. **2011**, *331*, 445-448.
12. Rau, H. Photoisomerization of Azobenzenes. *Photoreactive Organic Thin Films* **2002**, 3-47.
13. Yager, K. G.; Barrett, C. J. Novel Photo-Switching Using Azobenzene Functional Materials. *J Photochem Photobiol A Chem*. **2006**, *182*, 250-261.
14. Khan, A.; Kaiser, C.; Hecht, S. Prototype of a Photoswitchable Foldamer. *Angew Chem Int Ed Engl*. **2006**, *45*, 1878-1881.
15. Gelebart, A. H.; Jan Mulder, D.; Varga, M.; Konya, A.; Vantomme, G.; Meijer, E.; Selinger, R. L.; Broer, D. J. Making Waves in a Photoactive Polymer Film. *Nature*. **2017**, *546*, 632-636.
16. Chen, X.; Li, H.-X.; Zhang, Z.-Y.; Zhao, W.; Lang, J.-P.; Abrahams, B. F. Activation and Amplification of the Third-Order Nlo and Luminescent Responses of a Precursor Cluster by a Supramolecular Approach. *Chem Commun*. **2012**, *48*, 4480-4482.
17. Xue, X.; Wang, H.; Han, Y.; Hou, H. Photoswitchable Nonlinear Optical Properties of Metal Complexes. *Dalton Trans*. **2018**, *47*, 13-22.
18. Liaros, N.; Couris, S.; Maggini, L.; De Leo, F.; Cattaruzza, F.; Aurisicchio, C.; Bonifazi, D. NLO Response of Photoswitchable Azobenzene-Based Materials. *Chemphyschem*. **2013**, *14*, 2961-2972.
19. Bandara, H. M.; Burdette, S. C. Photoisomerization in Different Classes of Azobenzene. *Chem Soc Rev*. **2012**, *41*, 1809-1825.
20. Zhu, H.; Liu, M.; Zhou, J.; Xiao, X.; Wang, Y.; Chen, Z.; Xiao, S.; He, J. Two-Photon Absorption in Multi-Azobenzene Based Complexes Influenced by Photo-Isomerization. *Opt Mater*. **2022**, *133*, 112985.
21. Lin, T.; Peng, B.-X. Synthesis and Spectral Characteristics of Some Highly Soluble Squarylium Cyanine Dyes. *Dyes Pigments*. **1997**, *35*, 331-338.
22. Moreshead, W. V.; Przhonska, O. V.; Bondar, M. V.; Kachkovski, A. D.; Nayyar, I. H.; Masunov, A. E.; Woodward, A. W.; Belfield, K. D. Design of a New Optical Material with Broad Spectrum Linear and Two-Photon Absorption and Solvatochromism. *J Phys Chem C*. **2013**, *117*, 23133-23147.
23. Kubota, Y.; Tsukamoto, M.; Ohnishi, K.; Jin, J.; Funabiki, K.; Matsui, M. Synthesis and Fluorescence Properties of Novel Squarylium-Boron Complexes. *Org Chem Front*. **2017**, *4*, 1522-1527.
24. van Stokkum, I. H.; Larsen, D. S.; Van Grondelle, R. Global and Target Analysis of Time-Resolved Spectra. *Biochim Biophys Acta Bioenerg*. **2004**, *1657*, 82-104.
25. Hirose, Y.; Yui, H.; Sawada, T. Effect of Potential Energy Gap between the n-π* and the π-π* State on Ultrafast Photoisomerization Dynamics of an Azobenzene Derivative. *J Phys Chem A*. **2002**, *106*, 3067-3071.
26. Lednev, I. K.; Ye, T.-Q.; Hester, R. E.; Moore, J. N. Femtosecond Time-Resolved Uv-Visible Absorption Spectroscopy of Trans-Azobenzene in Solution. *J Phys Chem*. **1996**, *100*, 13338-13341.
27. Lednev, I.; Ye, T.-Q.; Matousek, P.; Towrie, M.; Foggi, P.; Neuwahl, F.; Umapathy, S.; Hester, R.; Moore, J. N. Femtosecond Time-Resolved Uv-Visible Absorption Spectroscopy of Trans-Azobenzene: Dependence on Excitation Wavelength. *Chem Phys Lett*. **1998**, *290*, 68-74.
28. Planells, M.; Pizzotti, M.; Nichol, G. S.; Tessore, F.; Robertson, N. Effect of Torsional Twist on 2nd Order Non-Linear Optical Activity of Anthracene and Pyrene Tricyanofuran Derivatives. *Phys Chem Chem Phys*. **2014**, *16*, 23404-11.
29. Maidur, S. R.; Patil, P. S.; Rao, S. V.; Shkir, M.; Dharmaprakash, S. M. Experimental and computational studies on second-and third-order nonlinear optical properties of a novel D-π-A type chalcone derivative: 3-(4-methoxyphenyl)-1-(4-nitrophenyl) prop-2-en-1-one. *Opt Laser Technol*. **2017**, *97*, 219-228.
30. Sheik-Bahae, M.; Said, A. A.; Wei, T.; Hagan, D. J.; Stryland, E. W. V. Sensitive Measurement of Optical Nonlinearities Using a Single Beam. *IEEE J Quantum Electron*. **1990**, *26*, 760-769.
31. Kovsh, D. I.; Hagan, D. J.; Stryland, E. W. V. Numerical Modeling of Thermal Refraction in Liquids in the Transient Regime. *Opt Express*. **1999**, *4*, 315-327.
32. Yang, J.; Song, Y. Direct observation of the transient thermal-lensing effect using the phase-object Z-scan technique. *Opt Lett*. **2009**, *34*, 157-159.
33. Yang, Y.; Wu, X.; Jia, J.; Shen, L.; Zhou, W.; Yang, J.; Song, Y. Investigation of Ultrafast Optical Nonlinearities in Novel Bis-Chalcone Derivatives. *Opt Laser Technol*. **2020**, *123*, 105903.
34. Yang, J.; Song, Y.; Wang, Y.; Li, C.; Jin, X.; Shui, M. Time-Resolved Pump-Probe Technology with Phase Object for Measurements of Optical Nonlinearities. *Opt Express*. **2009**, *17*, 7110-7117.
35. Boudebs, G.; Cherukulappurath, S. Nonlinear optical measurements using a 4f coherent imaging system with phase objects. *Phys Rev A*. **2004**, *69*, 053813.